

Stringent Test on Power Spectrum of Quantum Integrable and Chaotic Systems

A. L. Corps¹ and A. Relaño^{2,*}

¹*Departamento de Estructura de la Materia, Física Térmica y Electrónica,
Universidad Complutense de Madrid, Av. Complutense s/n, E-28040 Madrid, Spain*

²*Departamento de Estructura de la Materia, Física Térmica y Electrónica and GISC,
Universidad Complutense de Madrid, Av. Complutense s/n, E-28040 Madrid, Spain*

(Dated: December 21, 2024)

Quantum chaotic and integrable systems are known to exhibit a characteristic $1/f$ and $1/f^2$ noise, respectively, in the power spectrum associated to their spectral fluctuations. This can be exploited through the δ_n statistic. Theoretical expected values for both the integrable and the chaotic case have been derived and known for fifteen years. Recently [R. Riser, V. A. Osipov, and E. Kanzieper, *Power Spectrum of Long Eigenlevel Sequences in Quantum Chaotic Systems*, Phys. Rev. Lett. **118**, 204101 (2017)] a restriction on the mathematical conditions under which these curves should be obtained has been published, which seemingly supposed an invalidation of the traditional picture previously admitted for the power spectrum of this spectral statistic. This work treats the current scenario for the integrable and chaotic regularity classes separately. For the integrable case, we propose one protocol to follow if one wishes to successfully perform quantum spectral analyses based on formerly established results, which actually do remain valid. The theoretical expression for the chaotic case is only known up to a good approximation and is methodologically centered around the assumption that two-point correlations are enough to account for the dynamics. The abovementioned work introduced a new approach by which corrections beyond two-point correlations should be accommodated. By means of a rigorous statistical test on the chaotic theoretical curve, we show the original approximation provides a sufficiently safe and accurate description for this class of quantum systems and its correct application is indeed guaranteed for the vast majority of situations. Finally, we display an explicit transition from the chaotic to the integrable regime for a real, transiting, physical system, to which we apply the protocol we devise in this work, which yields excellent results.

I. INTRODUCTION

Quantum chaos is a relatively young discipline in Physics. Far from establishing a precise, clear definition for the term, the past century saw an identification of the energy level fluctuation properties of a given quantum system and the behavior of its classical analog for large time scales [1]. This resulted in a new picture by which one could understand the underlying classical dynamics of a quantum system by means of carefully analyzing its spectral fluctuations. For quantum systems whose classical analog is integrable, these were shown to be described by Poisson statistics by the pioneering work of Berry and Tabor in the 1970s [2], whereas for quantum systems for which the classical limit occurs in a fully chaotic nature, these correspond to the description given by the random matrix theory [3], as was correctly anticipated by Bohigas, Giannoni and Schmit in the 1980s [4]. According to this conjecture, level fluctuations in those quantum systems whose classical analog is chaotic will follow one of three classical ensembles, these being the Gaussian orthogonal ensemble (GOE), the Gaussian unitary ensemble (GUE) and the Gaussian symplectic ensemble (GSE). The agreement with one of the previous will strongly depend on the symmetries present in the Hamiltonian under consideration, which preserves the in-

dividuality of each system through an analysis based on statistical considerations.

Since then, different approaches have been developed and put to use to offer an accurate description of these spectral fluctuations. One of them is the nearest neighbor spacing distribution (NNSD), which essentially measures the intensity of level repulsion, to which chaoticity is directly related. The ratio of consecutive level spacings is another spectral statistic currently used due to the advantages that not requiring an unfolding process of the energy spectrum obviously offers. The reason for this lies in the fact that this distribution does not explicitly depend on the density of said energy levels [5].

The characterization of a quantum system in terms of the type of noise present in its power spectrum did not arrive until the beginning of the present century [6]. By considering the sequence of energy levels as a discrete time series, the conjecture read that quantum chaotic systems are characterized by an $1/f$ noise, ubiquitous throughout many complex systems, while for quantum integrable systems this noise becomes $1/f^2$. The hypothesized $1/f$ noise was then experimentally measured in Sinai microwave billiards [7] as well as in microwave networks [8], whereas an interpolating power-law $1/f^\alpha$, with $\alpha \in [1, 2)$, was implemented numerically for mixed classical dynamics systems [9]. This behavior in the power spectrum was afterwards conveniently exploited with the δ_n statistic, which keeps trace of long-range correlations of eigenlevels. With the central assumption that for a high enough number of levels in each spectrum the power

* Correspondence email address: armando.relano@fis.ucm.es

spectrum becomes exclusively dominated by two-point correlations, theoretical expressions for the power spectrum were derived for the chaotic GOE case in [10], as well as for the regular GDE case and for semiclassical systems, with the help of the random matrix theory. Moreover, results were shown to find solid support in numerical simulations, which expressed an excellent agreement with those. This approach was similarly applied to real physical systems (see [11] for a review).

More recently, a new study concerning the conditions under which the theoretical power spectrum needs to be derived has been published [12]. The work seems to invalidate the method shown in [10]—namely, that the power spectrum of a quantum system is solely determined by the spectral form factors associated to it. Indeed, according to [12], the power spectrum cannot be merely dominated by two-point correlations: to the contrary, as frequency is increased, this spectrum is increasingly influenced by spectral correlation functions of all orders or, equivalently, the power spectrum keeps record of all orders interactions. The main result given in the work is a parameter-free nonperturbative prediction for the power spectrum of the GUE ensemble. Although it is formally correct, we believe it is important to note here that the closed-form expression given in the work is quite cumbersome and mistakes can be easily incurred in. As for the other very often used ensembles, *no* mention of the GOE ensemble is made, and the comment they make on the functional form of the GDE theoretical expression, even though, again, formally correct, establishes a correction *virtually impossible* to obtain, since it would require a perfect unfolding procedure that introduces no spurious correlations. It turns out that these last two ensembles are the most frequently used to analyze experimental data since these correspond to the more frequent symmetries one finds in physical systems, while the GUE ensemble is quite rare in this sense. In conjunction with the previous remarks, this means that from a practical point of view the results devised in [10] remain to this day the best option in terms of applicability.

In this work we intend to supply a justification for the discrepancy appearing in the theoretical expression for the GDE case with respect to [10] and [12]. We explain how both equations are actually correct and justify how one needs to proceed to put a quantum integrable system power spectrum in correspondence with each one of them, providing a protocol that enables this purpose. Our main conclusion is that the requirements for the result given in [12] are almost impossible to fulfill, and that the applicability of the original expression, given in [10], happens to be much wider. Next, we perform a stringent test on the theoretical power spectrum for the GOE case given in [10] and conclude that, even if not strictly correctly derived for the reasons outlined in [12], it suffices to provide an excellent analysis of spectral data and can be used as an outstanding approximative tool to characterize the regularity class of a quantum system. Finally, we display an explicit transition from the chaotic to the

integrable case for a real physical system, which serves as proof that the expected theoretical results in [10] can be safely made use of.

II. NOTATIONAL CONVENTIONS AND DEFINITIONS

In this section we introduce some notation and definitions that will be constantly used without explicit mention throughout this work.

We consider sets of energy spectra consisting of N levels each, denoted by E_i , $i \in \{1, 2, \dots, N\}$. Let $\{E_i\}_{i=1}^N$ be a sequence of energies in ascending order, $E_i \geq E_j$ whenever $i \geq j$, for each spectrum in the ensemble. The *cumulative level density function* $N(E) \equiv \sum_{j=1}^N \Theta(E_j - E)$ is separated into a *fluctuating part*, $\tilde{N}(E)$ and a *smooth part*, $\bar{N}(E)$, which varies continuously with E . We make use of the latter for the *unfolding transformation*, by means of which a new sequence of dimensionless levels in ascending order $\{\epsilon_i\}_{i=1}^N$ is obtained via the mapping $E_i \mapsto \epsilon_i \equiv \bar{N}(E_i)$, $\forall i \in \{1, 2, \dots, N\}$. These *unfolded energies* can be used to study the statistical properties of different systems as well as different parts of the same spectrum accordingly, and remain valid for any quantum system, regardless of their regularity class.

The *nearest neighbor spacing* is defined to be the consecutive level difference $s_i \equiv \epsilon_{i+1} - \epsilon_i$, $\forall i \in \{1, 2, \dots, N-1\}$. The δ_n *statistic* is then taken to be $\delta_n \equiv \sum_{i=1}^n (s_i - \langle s \rangle) = \epsilon_{n+1} - \epsilon_1 - n$, $\forall n \in \{1, 2, \dots, N-1\}$, and represents the deviation of the excitation energy of the $(n+1)$ -th unfolded level from its mean value in an equispaced spectrum, $\langle \epsilon_n \rangle = n$. If we take n to be a discrete time index, a discrete Fourier transform can be applied to the statistic, thus yielding

$$\hat{\delta}_k \equiv \mathcal{F}[\delta_n] = \frac{1}{\sqrt{N}} \sum_{n=0}^{N-1} \delta_n \exp\left(\frac{-2\pi i k n}{N}\right) \in \mathbb{C}. \quad (1)$$

In Fourier space, we will also denote the N -rescaled frequencies by $\omega_k \equiv 2\pi k/N$, for each $k \in \{1, 2, \dots, N-1\}$. Real variables are associated to the subscript n , whilst for complex variables in Fourier space this identification occurs with the subscript k , although in some instances ω_k will indistinctly play a more useful role. All of them are considered discrete.

The δ_n *power spectrum*, which is the object of interest to us, is then defined to be the square modulus of the Fourier transform $\hat{\delta}_k$, that is, $P_k^\delta \equiv \left|\hat{\delta}_k\right|^2 \in \mathbb{R}$, $\forall k \in \{1, 2, \dots, N-1\}$, and allows for the study of the regularity of the system in terms of the density spectral fluctuations associated to it.

The positive integer $M \in \mathbb{N}$ will denote the *number of realizations* over which spectral and ensemble averages, denoted by $\langle \cdot \rangle_M$, will be carried. We will write $\langle \cdot \rangle$ whenever the theoretical value of such averages is being referred to.

To specify the distribution of an arbitrary random variable X , we will denote $X \sim Y$ to compactly mean that X has Y as a probability distribution. Note this has nothing in common with an asymptotic behavior. *Poisson distributions* are identified with exponential random variables $\text{Exp}(\lambda)$ with mean λ^{-1} , whereas the *normal distribution* with mean μ and variance σ^2 will be denoted by $\mathcal{N}(\mu, \sigma)$, with $\sigma \equiv \sqrt{\sigma^2}$ being the standard deviation associated with the variance σ^2 . The probability density and distribution functions of these random variables are denoted following the usual conventions.

Given a one-variable function $f = f(x)$, we will denote parametric dependence on y by the common expression $f(x; y)$. To lighten up the notation, subscripts will incidentally denote actual variables or parametric dependence, $f_x \equiv f(x)$, whenever these are used.

III. THE INTEGRABLE CASE

In this section we reason on the correct theoretical formula for the power spectrum of integrable quantum systems, we study how the introduction of the unfolding means a modification of such an expected value, and determine the conditions under which the usual spectral analysis needs to be considered.

A. Derivation of exact theoretical expression

Consider a spectrum made up of $N + 1$ energy levels. As expected, the δ_n statistic is defined $\delta_n = \sum_{i=1}^n (s_i - \langle s_i \rangle)$, $\forall n \in \{1, 2, \dots, N\}$. The mean value $\langle s_i \rangle$ is defined as an average over an ensemble of equivalent spectra. That is, if $s_i^{(k)}$ denotes the i -th spacing in the k -th realization, then

$$\langle s_i \rangle = \lim_{M \rightarrow \infty} \frac{1}{M} \sum_{k=1}^M s_i^{(k)} = 1, \quad \forall i \in \{1, \dots, N\}. \quad (2)$$

This mean value is not dependent on the value of i . Therefore, we shall denote $\langle s \rangle \equiv \langle s_i \rangle$, $\forall i$, where now $\langle s \rangle \equiv \lim_{N \rightarrow \infty} \frac{1}{N} \sum_{i=1}^N s_i$. It is worth remarking that

$$\langle s \rangle \neq \frac{1}{N} \sum_{i=1}^N s_i \equiv \langle s(N) \rangle, \quad (3)$$

where $\langle s(N) \rangle$ is a mean sample estimator, while $\langle s \rangle$ is the ensemble mean. From Eq. (2) we rewrite

$$\delta_n = \sum_{i=1}^n (s_i - 1), \quad n \in \{1, \dots, N\}. \quad (4)$$

In integrable systems the nearest neighbor spacings are not intrinsically correlated. This can be quantified by setting $s_i = \xi_i + 1$, where the random variables ξ_i are such that $\langle \xi_i \rangle = 0$ and $\langle \xi_i \xi_j \rangle = \delta_{ij}$, with δ_{ij} being the

Kronecker delta. It follows that for integrable systems the nearest neighbor spacings must verify the conditions

$$\langle s_i \rangle = 1, \quad (5a)$$

$$\langle s_i s_j \rangle = \delta_{ij} + 1. \quad (5b)$$

The second of the above, Eq. (5b), determines univocally how the nearest neighbor spacings are correlated in systems with this regularity class. Note that the definition of the probability density is not needed for this purpose. Therefore, what follows is valid no matter the probability density, even though we must only apply these results to Poisson statistics. Indeed, all non-integrable systems, whether they are chaotic or not, have nearest neighbor spacings where correlation exists.

More details on the calculation that follows are given in the Appendix. For integrable systems the (averaged) power spectrum of the δ_n statistic can be written

$$\langle P_k^\delta \rangle = \frac{1}{N} \sum_{\ell=1}^N \sum_{m=1}^N \langle \delta_\ell \delta_m \rangle e^{i\omega_k(\ell-m)}, \quad (6)$$

which applies to any frequency k . The correlation factor is given by

$$\langle \delta_\ell \delta_m \rangle = \min\{\ell, m\}. \quad (7)$$

Evaluating Eq. (6) affords

$$\langle P_k^\delta \rangle = \frac{1}{N} \sum_{\ell=1}^N \sum_{m=1}^N \min\{\ell, m\} e^{i\omega_k(\ell-m)}. \quad (8)$$

Performing the double sum over both ℓ and m yields

$$\langle P_k^\delta \rangle = \frac{1}{2 \sin^2\left(\frac{\pi k}{N}\right)} + \mathcal{O}\left(\frac{1}{N}\right). \quad (9)$$

Note that the expression given in [12] corresponds to the leading order of such integrable power spectrum. This is the only possible contribution only when $N \rightarrow \infty$. However, it is *not correct* that the theoretical power spectrum for integrable systems can be described by such a leading order term by itself for an arbitrary value of N , as has been suggested. The $1/f^2$ noise must be obtained for $k \ll N$ and $N \gg 1$ accordingly, since the neglected terms also do depend on k . It is under these circumstances that one would obtain the Maclaurin representation given by the inverse power-law

$$\langle P_k^\delta \rangle \simeq \frac{N^2}{2\pi^2 k^2} \propto \frac{1}{k^2}. \quad (10)$$

B. The role of the unfolding procedure

We now move on to examine the consequences of the process of unfolding. Even though the previous calculation is formally correct, the hypothesis under which it

has been derived are very strict in practical terms. The main reason for this is that the sequence of spacings is obtained after unfolding a set of levels characterized by a density of states that may very well be unknown. More importantly, Eq. (9) requires Eq. (5b) to be strictly verified to hold. This condition implies (see Appendix for details) $\langle \delta_\ell^2 \rangle = \ell$. Because every spectrum needs to be unfolded to generate the δ_n statistic, the following questions deserve to be asked: *Does the unfolding procedure really guarantee the complete verification of Eq. (5b)? Or, on the contrary, does it introduce some sort of spurious correlation in the statistical analysis?*

For the sake of simplicity, let us assume for a moment the smooth part of the states probability density, $\bar{\rho}(E)$, to be exactly known. Suppose as well that it is normalized such that

$$\int_{-\infty}^{\infty} dE \bar{\rho}(E) = N, \quad (11)$$

where N is the total number of levels in the spectrum. This is the case for the GDE, for which one has $\bar{\rho}(E) = 1/\sqrt{2\pi} \exp\{-x^2/2\}$. This is also the case where spurious effects are expected the least [13]. By definition, one has

$$\epsilon_1 = \bar{N}(E_1) \equiv \int_{-\infty}^{E_1} dE \bar{\rho}(E) \quad (12)$$

and

$$\epsilon_{N+1} = \bar{N}(E_{N+1}) \equiv \int_{-\infty}^{E_{N+1}} dE \bar{\rho}(E). \quad (13)$$

As a consequence, one clearly has $[\epsilon_1]_{\min} = 0$ as well as $[\epsilon_{N+1}]_{\max} = N + 1$. This argument can be generalized to assert that the minimum value of $\epsilon_i = \bar{N}(E_i)$ and the maximum value of $\epsilon_j = \bar{N}(E_j)$ are, respectively, $[\epsilon_i]_{\min} = 0$ and $[\epsilon_j]_{\max} = N + 1$, $\forall i, j \in \{1, \dots, N + 1\}$, where the equalities are strictly verified. Equivalently, one has $\epsilon_j \in (0, N + 1)$, where not all possible values are equally probable. Therefore, on calculating the δ_n statistic one finds, for $n = N$, $\delta_N = \epsilon_{N+1} - \epsilon_1 - N$. The maximum value of the above equation is then simply

$$[\delta_N]_{\max} = [\epsilon_{N+1}]_{\max} - [\epsilon_1]_{\min} - N = N + 1 - N = 1. \quad (14)$$

The result in Eq. (14) is in absolute contradiction with Eq. (5b) since, were they to hold, $\langle \delta_N^2 \rangle = N$, and δ_N would be a random variable with mean $\mu = 0$ and variance $\sigma^2 = N$. Observe that the statistic cannot be described by a random walk when the unfolding has been performed analytically on the original energy levels. Hence, we conclude that *the usual way to proceed with the unfolding process introduces spurious correlations in integrable systems. The relevance this bears on quantum chaotic systems is not so vital, because these are already intrinsically correlated.*

A convenient way to emulate these effects is to consider that, as a consequence of the spurious correlations, the

unfolding procedure acts on the sequence of spacings so as to

$$\frac{1}{N} \sum_{i=1}^N s_i = 1, \quad (15)$$

where the above equality is *exact*. In general, for a given set of spacings $\{s_i\}_{i=1}^N$ Eq. (15) is not strictly verified, but approximately.

A simple way to account for this effect is to redefine the nearest neighbor spacing to be

$$\tilde{s}_i \equiv \frac{s_i}{\langle s_i \rangle} = \frac{N s_i}{\sum_{k=1}^N s_k}, \quad \forall i \in \{1, \dots, N\}. \quad (16)$$

The set of spacings $\{\tilde{s}_i\}_{i=1}^N$ defined by Eq. (16) will be hereinafter called *reunfolding spacings*. If one performs an analogous calculation using the reunfolding spacings instead, this reads for $n = N$

$$\delta_N = \sum_{i=1}^N (s_i - 1) = N \langle s \rangle_M - N = N - N = 0. \quad (17)$$

This result is much closer to the property $[\delta_n]_{\max} = 1$, which has been understood to be a spurious consequence of the unfolding procedure, than it is to the ideal case where δ_N is a random variable with mean $\mu = 0$ and variance $\sigma^2 = N$.

An analogous statistic to the δ_n statistic can be naturally defined as that arising from the new sequence of spacings by the equivalence

$$\tilde{\delta}_n \equiv \sum_{i=1}^N (\tilde{s}_i - 1), \quad \forall n \in \{1, \dots, N\}. \quad (18)$$

We will refer to this statistic as the *corrected δ_n* . Associated with it is the new *corrected power spectrum*

$$\langle \tilde{P}_k^\delta \rangle \equiv \langle P_k^\delta \rangle = \frac{1}{N} \sum_{\ell=1}^N \sum_{m=1}^N \langle \tilde{\delta}_\ell \tilde{\delta}_m \rangle e^{i\omega_k(\ell-m)}, \quad (19)$$

which, after expansion, becomes

$$\langle \tilde{P}_k^\delta \rangle = \frac{1}{N} \sum_{\ell=1}^N \sum_{m=1}^N \left(\frac{N}{N+1} \min\{\ell, m\} - \frac{\ell m}{N+1} \right) e^{i\omega_k(\ell-m)}, \quad (20)$$

where the correlation factor is now given by

$$\langle \tilde{\delta}_\ell \tilde{\delta}_m \rangle = \frac{N}{N+1} \min\{\ell, m\} - \frac{\ell m}{N+1}. \quad (21)$$

Performing the corresponding double sum now yields

$$\langle \tilde{P}_k^\delta \rangle = \frac{1}{4 \sin^2(\frac{\pi k}{N})} + \mathcal{O}\left(\frac{1}{N}\right), \quad (22)$$

which differs from Eq. (9) by a factor of 2. Clearly, one has $\langle P_k^\delta \rangle = 2\langle \tilde{P}_k^\delta \rangle$. The leading order of Eq. (22) corresponds with the theoretical power spectrum for the integrable case derived in [10]. In the domain defined by the conditions $k \ll N$ and $N \gg 1$, one analogously has for the Maclaurin representation of Eq. (22) the known inverse square power-law

$$\langle \tilde{P}_k^\delta \rangle \simeq \frac{N^2}{4\pi^2 k^2} \propto \frac{1}{k^2}. \quad (23)$$

The calculation is shown at length in the Appendix.

C. Numerical evidence

To illustrate numerically the above results, we proceed as follows. For the following scenarios, we must keep in mind that we are interested in the best possible unfolding, that is, the one that introduces the least possible noise in our analysis. This requires making use of an analytical exact formula obtained for the cumulative density of states, \bar{N} . Since the starting probability distribution is a standard normal and we need it to be normalized to the number of levels participating in the unfolding process, we calculate

$$\begin{aligned} \bar{N}(E) &= N \int_{-\infty}^E dx \frac{1}{\sqrt{2\pi}} \exp\left(\frac{-x^2}{2}\right) \\ &= \frac{N}{2} \left[1 - \operatorname{erf}\left(\frac{-E}{\sqrt{2}}\right) \right], \end{aligned} \quad (24)$$

where $\operatorname{erf}(\cdot)$ is Gauss error function. Eq. (24) is the exact formula employed to find the unfolded levels in this part of the work. We simultaneously consider two different processes:

I Generate a vector A of dimension $N = 10^9$ whose entries are numbers coming from a standard normal distribution, that is, select a certain $A \in \mathcal{M}_{1 \times N}(\mathcal{N}(0, 1))$ whose entries, after reordering in ascending order if necessary, will be taken as the initial levels $\{E_i\}_{i=1}^N = \{(A)_{1,i}\}_{i=1}^N$. Next, the sequence is unfolded to obtain the list of levels in ascending order $\{\epsilon_i\}_{i=1}^N = \{\bar{N}(E_i)\}_{i=1}^N$. *Note the unfolding is only performed once.* Fix $M = 10^6$. Partition the set of unfolded levels into M sets of energies consisting of $N/M = 10^3$ levels each, that is, construct explicitly the M sets of levels $\left\{ \left\{ \epsilon_{i+(j-1)N/M} \right\}_{i=1}^{N/M} \right\}_{j=1}^M$. We expect the spurious effects introduced by the unfolding process to be less important for this case, the reason being that those should have an effect on large distance correlations. Because the unfolded spectrum has been split into spectra with relative length $(N/M)/N = 1/M = 10^{-6}$, it stands to reason to expect them not to play such an important role. Note that these spurious effects should manifest primarily on the leftmost and rightmost eigenlevels in the spectrum for each realization, and this process explicitly assigns these edges a

slight weight over the total ensemble under consideration. Obtain the averaged power spectrum $\langle P_k^\delta \rangle_M$. Conclude it is accurately described by Eq. (9). Construct the random variable δ_n^2 and find $\langle \delta_n^2 \rangle_M$. Compare the result with the expected value Eq. (7) with $\ell = m \equiv n$, that is,

$$\langle \delta_\ell \delta_m \rangle \Big|_{\ell=m=n} = \langle \delta_n^2 \rangle = n. \quad (25)$$

Observe this second-order moment is expected to behave linearly and to grow unboundedly as n grows.

II Generate a vector A of dimension $N = 10^3$ whose entries are numbers coming from a standard normal distribution, that is, select a certain $A \in \mathcal{M}_{1 \times N}(\mathcal{N}(0, 1))$ whose entries, after reordering in ascending order if necessary, will be taken as the initial levels $\{E_i\}_{i=1}^N = \{(A)_{1,i}\}_{i=1}^N$. Proceed as in **I**, but *do not partition the set of energies*. Repeat and average over $M = 10^6$ realizations. *It is noteworthy that the unfolding procedure is considered exactly M times now.* This means all M spectra and the eigenlevels located at their leftmost and rightmost positions will suffer from spurious correlations implicitly introduced by the unfolding process, which will be present throughout the whole ensemble. Find the averaged power spectrum $\langle P_k^\delta \rangle_M$. Conclude it is governed by Eq. (22). Construct the random variable δ_n^2 and find $\langle \delta_n^2 \rangle_M$. Compare the result with the expected value Eq. (21) with $\ell = m \equiv n$, that is,

$$\langle \tilde{\delta}_\ell \tilde{\delta}_m \rangle \Big|_{\ell=m=n} = \langle \tilde{\delta}_n^2 \rangle = \frac{nN}{N+1} - \frac{n^2}{N+1}. \quad (26)$$

Observe this second-order moment is expected to be parabolic and to reach its maximum value when $n = N/2$.

The previous steps can be performed algorithmically to obtain the desired results, which are, in essence, the mean δ_n^2 over the total ensemble and the averaged integrable power spectrum for each different process above detailed. These are shown in Figs. 1 and 2.

In Fig. 1, we contrast the simulated data $\langle \delta_n^2 \rangle_M^i$, $i \in \{\mathbf{I}, \mathbf{II}\}$ for the processes **I** and **II** with the theoretical expected curves. We observe the outstanding agreement with which $\langle \delta_n^2 \rangle_M^{\mathbf{I}}$ is put in correspondence with Eq. (25), while this is analogously true for $\langle \delta_n^2 \rangle_M^{\mathbf{II}}$ and Eq. (26), as we had anticipated. Fig. 1 allows to conclude that, indeed, the nature of spurious correlations can be greatly modified by performing the previous steps, and this relies, basically, on altering the region of the spectrum where the unfolding is permitted to add information that was initially not there.

In Fig. 2, we confirm the results just recently discussed. As one would expect, different correlation functions are associated with different power spectra, and we have managed to make $\langle P_k^\delta \rangle_M^{\mathbf{I}}$ coincide with the results predicted by Eq. (9), as explained in **I**, whereas $\langle P_k^\delta \rangle_M^{\mathbf{II}}$ agrees with Eq. (22), according to **II**. In both cases we observe how the numerical data are equally outstandingly well described by the theoretical curve to which they are related.

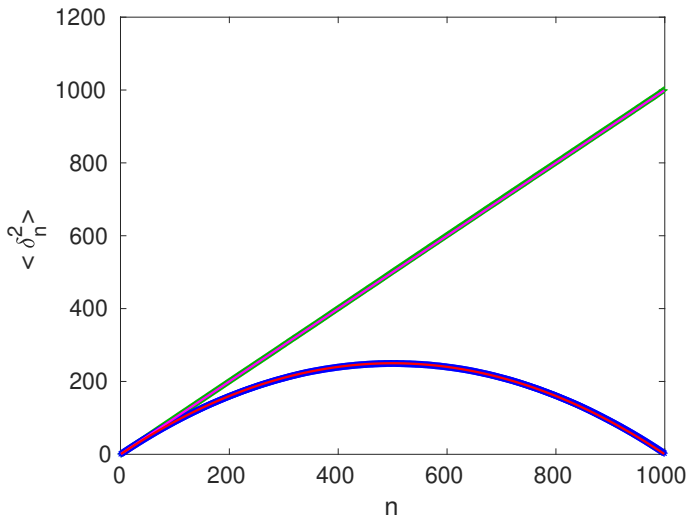


FIG. 1. (Color online) Theoretical $\langle \delta_n^2 \rangle$ for GDE Eqs. (25) (top, magenta solid line) and (26) (bottom, red solid line) compared to numerical averages consisting of 10^6 spectra with $N = 10^3$ levels each obtained following processes **I** (top, green solid points) and **II** (bottom, blue solid points).

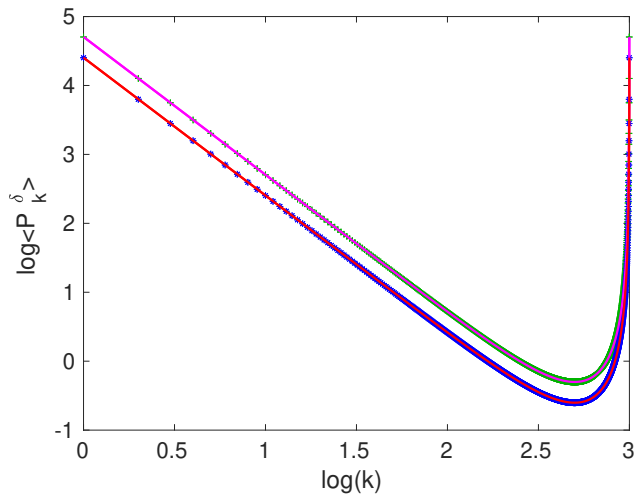


FIG. 2. (Color online) Theoretical $\langle P_k^\delta \rangle$ for GDE Eqs. (9) and (22) (top and bottom solid lines) compared to numerical averages consisting of 10^6 spectra with $N = 10^3$ levels each obtained following processes **I** (+ symbols) and **II** (* symbols).

As has been shown, in spite of the fact that the result given in [12] is, by all means, correct, the unfolding procedure very often followed introduces spurious correlations that act on the unfolded sequence such that they are described by the theoretical expression in [10]. We note that, for any given spectrum coming from a calculation or an experiment, it is very frequent to proceed with the statistical analysis *without partitioning* our sample of eigenlevels. Our results prove that, in all those cases,

one needs to take the results in [10] into consideration to perform a successful investigation.

We would like to end this section after a relevant remark. The role the unfolding procedure plays in the study of quantum integrable systems, namely, the introduction of spurious correlations that manifest throughout the whole spectrum, has universal implications that apply to other spectral statistics that are usually jointly considered to make a decision about the regularity of a quantum system. For the *number variance*

$$\Sigma^2(L) \equiv \langle (n(E, L) - L)^2 \rangle, \quad (27)$$

where $L \gg 1$ is the size of an interval in \mathbb{R} and $n(E, L)$ denotes the number of levels in such an interval at energy E , the theoretical machinery predicts a linear expected value for the integrable case

$$\Sigma_{\text{Int}}^2(L) = L. \quad (28)$$

Similarly, long-range correlations of level spacings can also be characterized by means of the Dyson-Mehta *spectral rigidity*,

$$\Delta_3(E_0, L) \equiv \frac{1}{L} \min_{\alpha, \beta \in \mathbb{R}} \int_{E_0}^{E_0+L} dE [N(E) - \alpha E - \beta]^2, \quad (29)$$

for which the integrable regime is governed by the like-wise linear expression

$$\Delta_3^{\text{Int}}(E_0, L) = \frac{L}{15}. \quad (30)$$

As can be seen in Eqs. (28) and (30), these spectral statistics seem to share a commonality with the δ_n^2 in that the regular regime takes on a linear form as well. This is due to the mathematical hypothesis under which these results have been derived, consisting of completely uncorrelated level spacings (see, preferably, [3]). This was to be expected. However, careful accommodation of the spurious correlations, trademark of the unfolding process, implies that this behavior will suffer a modification that goes in the same direction as that of Eq. (26), which means the linear structure will be severely influenced by correlations that should in principle not exist in an integrable quantum system, and deviations will, too, occur for both $\Sigma_{\text{Int}}^2(L)$ and $\Delta_3^{\text{Int}}(E_0, L)$, meaning these will no longer be described by such a simple linear functional form. This has already been justified for the δ_n^2 statistic through the realization that level spacings cease to be uncorrelated as a consequence of the unfolding transformation. It directly follows that, when uncorrelation is also violated for the other two statistics, the same conclusion must be reached.

IV. THE CHAOTIC CASE

The main purpose of this section is to show that the theoretical expression for the averaged power spectrum

$\langle P_k^\delta \rangle$ derived in [10], making use of spectral form factors under the hypothesis that two-point correlations dominate the dynamics, is sufficient to obtain a correct representation of the behaviour of the system. Indeed, as suggested in [12], the procedure to follow if one wishes to find the correct theoretical expression needs to take into account the reality that the power spectrum is increasingly influenced by spectral correlation functions of all orders. Notwithstanding, such an exact formula has not been deduced as of yet, and in said work no explicit mention of the structure this expression should have is made. Therefore, it is our goal to show here that, even if the initial hypothesis that two-point correlations can be used to describe the power spectrum should not hold, the numerical agreement is remarkably good, thus justifying its use to study the chaotic nature of a quantum system.

A. Influence of the number of realizations

Explicitly, the two-point correlation theoretical expression for quantum chaotic systems, within the context of RME, takes on the free-parameter form

$$\langle P_k^\delta \rangle = \frac{N^2}{4\pi^2} \left[\frac{K\left(\frac{k}{N}\right) - 1}{k^2} + \frac{K\left(1 - \frac{k}{N}\right) - 1}{(N - k)^2} \right] + \frac{1}{4 \sin^2\left(\frac{\pi k}{N}\right)} - \frac{1}{12}, \quad (31)$$

where $k \in \{1, 2, \dots, N - 1\}$, N denotes the size of each spectrum in the ensemble over which the average has been performed, and the spectral form factor, K , for the GOE case admits the representation

$$K(\tau) = \begin{cases} 2\tau - \tau \log(1 + 2\tau), & \tau \leq 1 \\ 2 - \tau \log\left(\frac{2\tau + 1}{2\tau - 1}\right), & \tau \geq 1 \end{cases} \quad (32)$$

which will be put in comparison with two sets of numerical data. We will consider simultaneously an ensemble of $M = 10^2$ and $M = 10^6$ GOE matrices of dimension $N = 10^3$ each. The corresponding power spectra for the δ_n statistic is then calculated as follows. We first evaluate the smooth cumulative density function \overline{N} at the energy levels $\{E_i\}_{i=1}^N$. We invoke the properties of the GOE ensemble and make use of its exact free-parameter cumulative density obtained, for instance, in [1], that is,

$$\overline{N}(E) = \frac{E}{2\pi} \sqrt{2N - E^2} + \frac{N}{\pi} \arctan\left(\frac{E}{\sqrt{2N - E^2}}\right) + \frac{N}{2}, \quad |E| \leq \sqrt{2N}, \quad (33)$$

$\overline{N}(E) = 0$, if $E < \sqrt{2N}$, and $\overline{N}(E) = N$, if $E > \sqrt{2N}$, in such a way that the new unfolded levels are uniquely determined. This corresponds to the so-called Wigner's

semicircle law. We note that the first and last levels of the original sequence of energies have been eliminated to avoid dealing with spurious effects arising from it. It is worth observing that the sequence $\{\epsilon_i\}_{i=1}^N$ is in this case perfectly calculated: any attempt to find it by fitting to any polynomial would result in a noisy set of unfolded levels, and this is true independently of the adequacy of the polynomial. We then construct the nearest neighbor spacings as $s_i \equiv \epsilon_{i+1} - \epsilon_i$, $\forall i \in \{1, 2, \dots, N - 1\}$, from which the expression for the δ_n statistic as well as its power spectrum P_k^δ is a straightforward matter. In Figs. 3 and 4, we display the parameter-free prediction with the results of numerical simulations for these sets of spectra. Note that the simulated points have been represented with a dashed line for viewing purposes only.

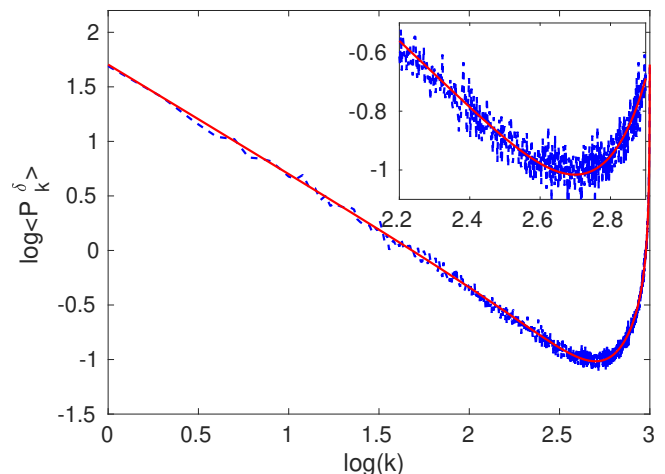


FIG. 3. (Color online) Theoretical power spectrum $\langle P_k^\delta \rangle$ of the δ_n function for GOE (solid line), compared to numerical averages consisting of 10^2 spectra with $N = 10^3$ levels each (dashed line).

Fig. 3 clearly establishes the impossibility of ruling out the disagreement between theoretical and simulated points because of the noisy nature of the spectral fluctuations, whilst we observe a discrepancy in the second case, Fig. 4, for high-lying frequencies, $2.5 \lesssim \log(k) \lesssim 2.8$, as well as for low-lying ones, $0 \lesssim \log(k) \lesssim 0.5$. This serves the initial purpose of suggesting that as the number of realizations involved in the average increases, the accordance of the numerical data and the theoretical curve will decrease. The same conclusion was reached in [12].

In Fig. 5 we show the histogram representing the probability density of the random variable $\langle P_k^\delta \rangle$ for the frequency $k = 400$ plotted against a Poisson probability density with mean $\langle P_{400}^\delta \rangle$. The agreement is remarkable, so much so that we have only been able to clearly show one of said two curves. The behaviour is analogous for any other frequency k , so that in general the random variable $\langle P_k^\delta \rangle$ for quantum chaotic systems is distributed

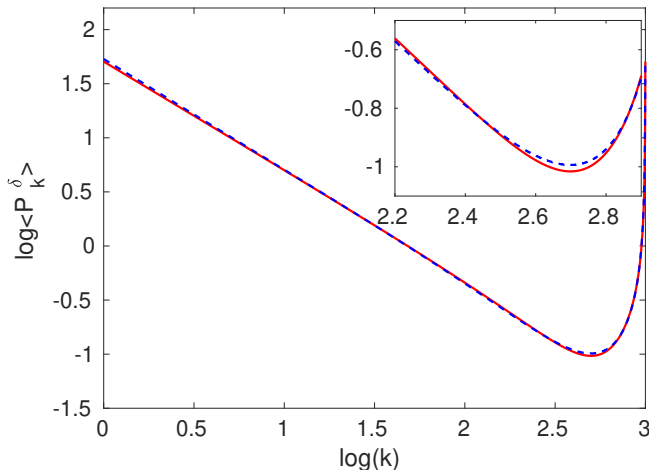


FIG. 4. (Color online) Theoretical power spectrum $\langle P_k^\delta \rangle$ of the δ_n function for GOE (solid line), compared to numerical averages consisting of 10^6 spectra with $N = 10^3$ levels each (dashed line).

as

$$\langle P_k^\delta \rangle \sim \text{Exp} \left(\frac{1}{\langle P_k^\delta \rangle} \right). \quad (34)$$

One quickly realizes that since for the chaotic $\langle P_k^\delta \rangle$ the statistical mode and the mean value are reasonably far from each other, a single realization will not be representative of the theoretical distribution. This implies that in order to obtain statistically significant results one must go on to consider averages over many realizations.

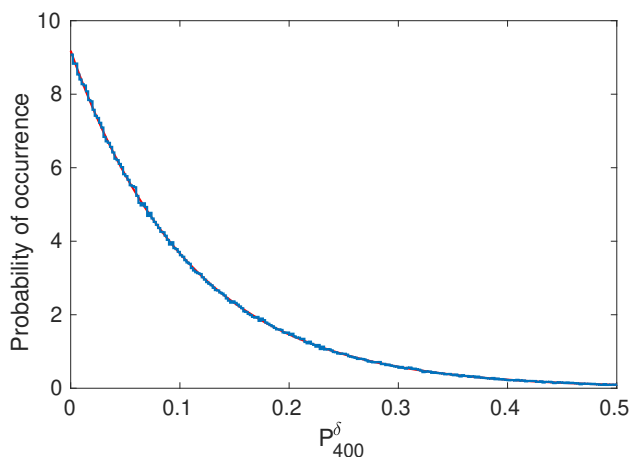


FIG. 5. (Color online) Probability density for the random variable P_{400}^δ . Numerical simulations carried with $M = 10^6$ spectra of $N = 10^3$ levels each.

B. Significance test on two-point power spectrum result

We wish to obtain an upper bound for the number of realizations for which the numerical discrepancy cannot be substantiated in terms of statistical significance. This can be accomplished by making use of standard probability considerations. Let M be a positive integer. For a large enough number of realizations M , we will search for an estimate of the mean $\langle P_k^\delta \rangle$ and the variance $\sigma_{P_k^\delta}^2$. Since the results represented in Fig. 4 have been calculated with an ensemble of $M = 10^6$ spectra, they qualify as a good starting point. Let P_k^δ be a random variable with mean $\langle P_k^\delta \rangle$ and variance $\sigma_{P_k^\delta}^2$. By the well-known central limit theorem, the probability distribution of the mean estimator random variable $\langle P_k^\delta \rangle_M \equiv \frac{1}{M} \sum_{i=1}^M P_k^{(i)}$ is found to be

$$\langle P_k^\delta \rangle_M \sim \mathcal{N} \left(\langle P_k^\delta \rangle_\infty, \frac{\sigma_{P_k^\delta}^2}{\sqrt{M}} \right), \quad (35)$$

where $\langle P_k^\delta \rangle_\infty \equiv \mu_M$ corresponds to the mean value for the power spectrum calculated with the ensemble of 10^6 spectra, $\sigma_{P_k^\delta} \equiv \sqrt{\sigma_{P_k^\delta}^2}$ is now the standard deviation associated with it, $\sigma_M \equiv \sigma_{P_k^\delta} / \sqrt{M}$, and $1 \ll M \lesssim 10^6$ is an arbitrary number of realizations. The next step is therefore to investigate this new distribution as a function of M . It follows from Eq. (35) that the probability density function for the random variable $\langle P_k^\delta \rangle_M$ is simply given by the two-parameter expression

$$\rho_M(x) = \frac{1}{\sigma_M \sqrt{2\pi}} \exp \left[-\frac{(x - \mu_M)^2}{2\sigma_M^2} \right]. \quad (36)$$

Note, however, that $\mu_M \neq \mu_M(M)$, since this value is fixed as a constant regardless of the value of M .

To assess how incompatible the numerical data are with the theoretical formula for the GOE case we will immediately implement the p -values. We will assume the theoretical formula to be incorrect whenever $p < 0.05$, that is, we will consider the adjustment to the theoretical curve to be due to chance. Otherwise, whenever $p \geq 0.05$, the agreement will be taken statistically substantiated.

Let T_k denote the theoretical value for $\langle P_k^\delta \rangle_\infty$ given by Eq. (31). The p -value for each value of M , $p(k; M)$, is then taken to be

$$p(k; M) = \begin{cases} \int_{T_k}^{\infty} dx \rho_M(x), & T_k \geq \langle P_k^\delta \rangle_\infty, \\ \int_{-\infty}^{T_k} dx \rho_M(x), & T_k \leq \langle P_k^\delta \rangle_\infty. \end{cases} \quad (37)$$

Since for each case the result depends strongly on M , this can be used to study the function $p(k; M)$ for certain values of the number of realizations. This is plotted in Fig. 6 for, from top to bottom, $M = 10, 30, 100, 300, 1000, 3000, 10000, 30000$. The value $p =$

0.05 has been represented as the upper limit for which the theoretical curve remains invalid. To better understand this result, we have also plotted the values of the relative error $|T_k - \langle P_k^\delta \rangle_{10^6}|/T_k$ as a function of the frequency in Fig. 7. This is the relative error with respect to the expected value for the ensemble of $M = 10^6$ spectra that we chose to establish an ensemble estimator via the central limit theorem, which means it will be representative for $1 \ll M \lesssim 10^6$ as well.

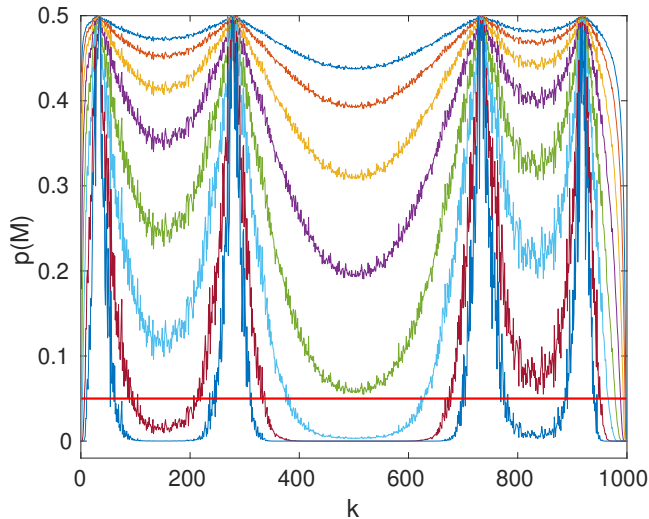


FIG. 6. (Color online) Values of $p(M)$ for, from top to bottom, $M = 10, 30, 100, 300, 1000, 3000, 10000, 30000$. The value $p = 0.05$ has been represented (red solid line) as the upper limit for which the theoretical curve remains invalid.

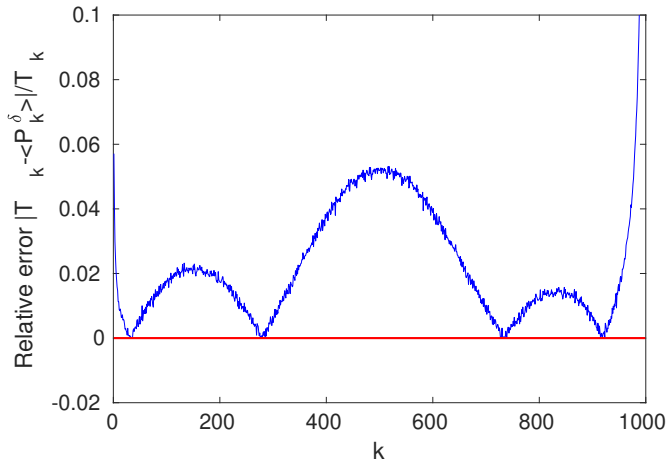


FIG. 7. (Color online) Relative error with respect to the theoretical values for the case in which $M = 10^6$.

We conclude that for numbers of realizations $M \lesssim 10^3$, for all frequencies the inequality $p(M) > 0.05$ is verified and, as a consequence, in all these cases it is reliable to take the agreement between theoretical expression and

Protocol for spectral statistical analysis

-
- Step 1.** Unfold each spectrum individually, either analytically or numerically. If a complete spectrum with N levels is divided into M spectra with N/M levels each, then unfold each spectrum of length N/M separately too.
- Step 2.** Proceed with the spectral analysis, and compare the results it yields with the expected expressions in [10].
-

TABLE I. Suggested protocol to follow for the unfolding procedure so that the analyzed results can be compared with the theoretical expressions for the power spectrum of quantum integrable and chaotic systems in [10].

numerical data as statistically significant. However, for values $M \gtrsim 10^3$ this is not guaranteed, and we observe indeed that $p(M)$ tends to zero for these cases in the same way the relative error increases for certain frequencies. For large enough values of M , the theoretical expression becomes valid only for a few points corresponding to the minima of the relative error. In particular, it is *only* in the large- M limit that the result is completely unacceptable for all frequencies, as exemplified by

$$\lim_{M \rightarrow \infty} p(k; M) = 0, \quad \forall k \in \{1, 2, \dots, N-1\}. \quad (38)$$

Also worth remarking is the observation that the maximum error occurs for the Nyquist frequency $\omega_{k_{Ny}} \equiv \pi$, i.e., $k_{Ny} \equiv N/2$.

This implies that the theoretical result derived in [10], even though not fully correct, can be viewed as an extraordinary tool to analyze the chaoticity of a quantum system, so long as the realizations are not too many. Our results indicate that the corresponding expressions can thus be safely used. It is obvious that an explicit, easily applicable, closed-form expression for GOE is desirable, but it would not yield further significant improvements in spectral analyses. Indeed, the circumstances under which these results could be important constitute quite a small set of conditions. This manifests itself blatantly when one realizes that the general picture is that in which one may reasonably have only one set of eigenlevels with a relatively small size when compared with the dimension scales considered in this work.

With all the previous conclusions available to us, we propose one procedure to correctly perform any power spectrum analysis in Tab. I.

V. TRANSITION IN A REAL PHYSICAL SYSTEM

In this section we apply the previous protocol to a physical system that transits from the chaotic regularity class to the integrable one.

The model under consideration is a Heisenberg spin-1/2 chain. Such a model has been proved to transit from

integrability to chaos using the nearest neighbor spacing distribution [14] as well as the the ratio of consecutive level spacings distribution [15]. Here, we will concentrate on the transition as seen by the δ_n statistic.

The Hamiltonian of the Heisenberg spin-1/2 chain model is given by

$$H = \sum_{n=1}^L \omega_n S_n^z + \varepsilon S_d^z + \sum_{n=1}^{L-1} J \hat{S}_n \cdot \hat{S}_{n+1}, \quad (39)$$

where L is the number of sites, $\hbar = 1$ and $\hat{S}_n \equiv \vec{\sigma}_n/2$ are the spin operators located at site n with $\vec{\sigma}_n$ being the Pauli spin matrices at that exact site. We briefly comment on the meaning of each of the terms in Eq. (39). The first term describes the Zeeman splitting of each spin n as a consequence of the static magnetic field in the z -direction. In general, each ω_n is a random variable belonging to certain probability distribution. A site d is called a defect if all the other sites are assumed to have the same energy splitting $\omega_n = \omega$ except the site d , where the splitting is $\omega + \varepsilon$ instead. Finally, two possible couplings between the nearest neighbor spins are described by the last term of Eq. (39). The first one is simply the diagonal Ising interaction, while the second is the off-diagonal flip-flop term, which is responsible for excitation propagation in the chain. Also, the chain is taken to be isotropic since J is a constant that quantifies both the coupling strength between the Ising interaction and that of flip-flop term. Only two-body interactions can take place in this chain.

For our simulation, the defect energy difference has been chosen to vanish, $\varepsilon = 0$, and the static magnetic field is random. We have taken $J = 1$ and the number of sites $L = 13$. In other words, we will study the transition given rise by the one-parameter Hamiltonian

$$\mathcal{H} \equiv H(\omega_n, \varepsilon = 0) = \sum_{n=1}^{13} \omega_n S_n^z + \sum_{n=1}^{12} \hat{S}_n \cdot \hat{S}_{n+1}. \quad (40)$$

Each realization consists of $L = 13$ random numbers whose probability distribution we have decided to choose $\omega_n \sim \mathcal{N}(0, \omega)$, $n \in \{1, 2, \dots, 13\}$, where $\omega \in \{0.2, 0.4, 0.6, \dots, 50.0\}$ or, equivalently, $\omega = 0.2q$, where $q \in \{1, 2, \dots, 250\}$. Since $[H, \hat{S}_z] = 0$, we consider the sector with $\hat{S}_z = -1/2$. It is advantageous to work with this model because it allows for an average over a large number of realizations after obtaining the energy spectrum associated with \mathcal{H} for each one of them. In this case,

the dimension of the Hilbert space is $d = \binom{13}{6} = 1716$.

The size of each spectrum has been therefore chosen $N = 1716$, and we have simulated $M = 2000$ realizations. We have excluded the first and last 40 levels both before and after the unfolding process, in order to prevent spurious effects from happening in our analysis. The polynomial to which we have fitted the original set of energies $\{E_i\}_{i=1}^N$ to obtain the unfolded sequence $\{\epsilon_i\}_{i=1}^N$

was taken to be of degree 10, which means the smooth part of the cumulative density function was of the form $\overline{N}(x) = \sum_{k=1}^{10} a_k x^k$, with coefficients $\{a_k\}_{k=1}^{10}$ that resulted from the best possible fit to the sequence $\{E_i\}_{i=1}^N$. Then, it is straightforward to evaluate $\overline{N}(x)|_{x=E_i} = \epsilon_i$, $\forall i \in \{1, 2, \dots, N\}$. Note we have stuck to the protocol we proposed in Table I to analyze quantum spectra at all times. The results are shown in Fig. 8 for the noise parameter values $\omega \in \{0.2, 0.4, 0.8, 1.6, 3.0, 6.0, 10.0, 50.0\}$ in panels (a) to (h), respectively. We observe how a smooth transition is accomplished from the chaotic case, in panel (a), to the integrable case, in panel (h). The values of ω have been selected so that the evolution happens gradually. Note however that the system cannot be said to be completely chaotic for $\omega = 0.2$ since the simulated power spectrum deviates from its theoretical GOE curve for the low-lying frequencies $0.4 \lesssim \log(k) \lesssim 1.1$. The agreement between simulated data and expected theoretical GDE result, Eq. (22), is very satisfying already for $\omega = 10.0$.

Let us denote the expected value Eq. (22) by $\langle P_k^\delta \rangle_{\text{GDE4}}$ for a moment. If we make explicit the dependence of the simulated $\langle P_k^\delta \rangle_M$ on the parameter ω and write $\langle P_k^\delta \rangle_M(\omega)$ accordingly to signify the averaged power spectrum for each value of ω in the set specified, we observe that our results are compatible with

$$\lim_{\omega \rightarrow \infty} \langle P_k^\delta \rangle(\omega) = \langle P_k^\delta \rangle_{\text{GDE4}}, \quad \forall k \in \{1, 2, \dots, N-1\} \quad (41)$$

In other words, the simulated data tend to the expected curve $\langle P_k^\delta \rangle_{\text{GDE4}}$ as the value of ω is increased, which corresponds to the integrable regime, but under no circumstances do they go beyond such a curve. This can be seen as a limit process where the limiting value is given by Eq. (22). The theoretical value Eq. (9) has been added to panel (h) as well in order to graphically clarify that if one were to make use of such an expression to study the exact same transition an intermediate conclusion, belonging *neither* in the integrable *nor* in the chaotic case, would be reached. This would be in clear contradiction with the dynamics transition that is however well-established for this system, thus resulting in an obviously wrongful verdict.

We conclude the equations derived in [10] can be safely used to characterize the regularity of real complex many-body quantum systems, such as atoms, nuclei, spin chains, quantum dots and so on through the δ_n power spectrum.

VI. CONCLUSIONS

The study of quantum many-body regularity class can be undertaken by means of spectral statistics. One of such statistics frequently used in the analysis is the δ_n , whose power spectrum is of interest because it relates the

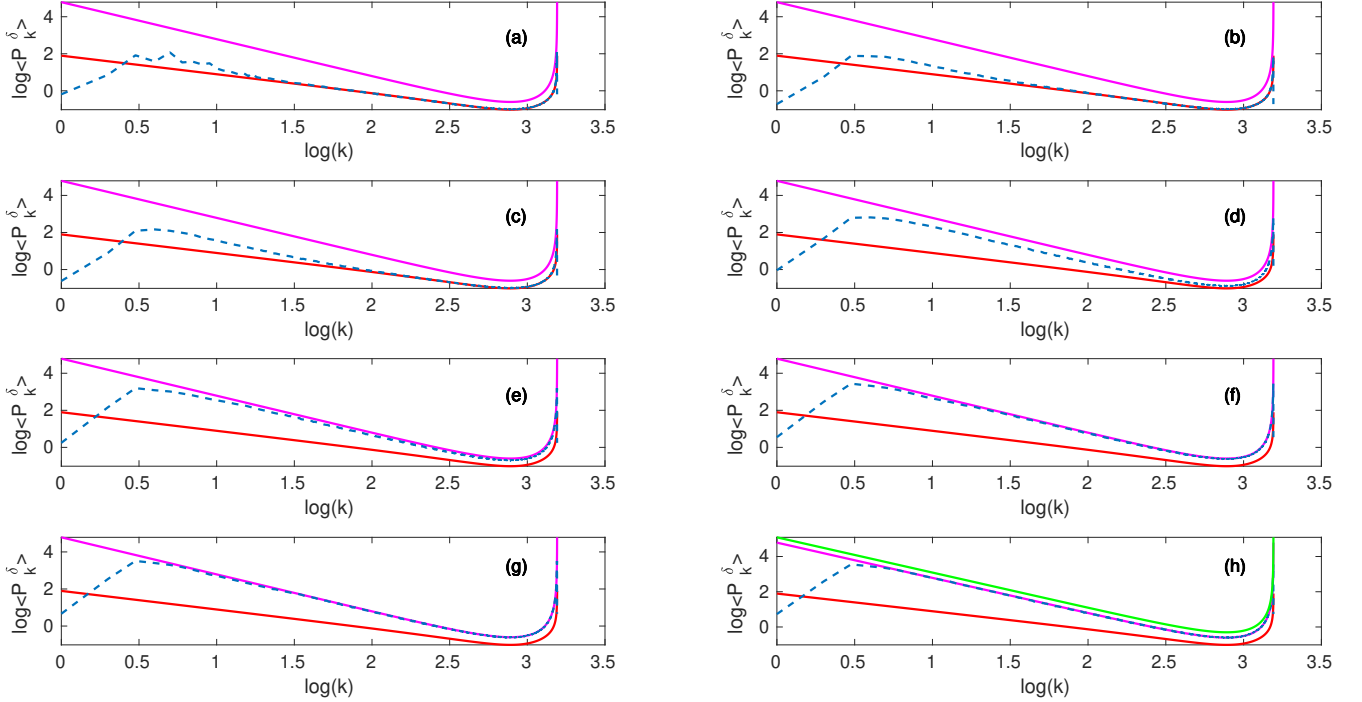


FIG. 8. (Color online) Transition of the system with eigenvalues obtained from \mathcal{H} , Eq. (40), from the chaotic, (a), $\omega = 0.2$, to the integrable, (h), $\omega = 50.0$, regime (dashed lines). Plotted against them are the theoretical power spectrum curve for GOE given in Eq. (31) (red solid line) and the leading order of the theoretical power spectrum for GDE given in Eq. (22) (magenta solid line). Additionally, Eq. (9) has been represented in panel (h) (green solid line) for comparison. An average over $M = 2000$ spectra with $N = 1716$ levels each has been performed.

degree of chaoticity of a system with an universal noise of the form $1/f$ and $1/f^2$ for chaotic and integrable systems, respectively. Theoretical representations for the expected values of the power spectra have been derived in the past. Our interest has been focused on the classical ensembles that describe the most frequent physical systems, that is, GDE and GOE.

In this work we have established the role that the process of unfolding plays in spectral analysis, namely, that it introduces spurious correlations. However, since level repulsion for quantum chaotic dynamics means in these systems correlations already exist, this is of utter importance for quantum integrable systems only, since in principle correlations should not be present in their characterization. A consequence that cannot go unnoticed is that, as a result, the GDE power spectrum obtained by the usual procedure of unfolding deviates from its expected theoretical expression by a factor of 2, which makes itself evident in the analysis. This effect cannot be escaped, *not even by proceeding with a perfect, exact, analytic unfolding transformation*. In this work, we have therefore provided a protocol to follow if one wishes to succeed in comparing quantum integrable power spectra with theoretical values.

The GOE case is doubtlessly less fortunate, since we are still lacking an exact representation for its theoretical power spectrum expected value, which needs to be found by considering correlations to all orders. This means the approximate form derived in [10] is currently our best possible alternative. By performing a stringent, rigorous statistical test on this result, we have proved that this can be regarded as an excellent tool to guarantee that a quantum system belongs in the chaotic class, and can be safely made use of in a wide range of situations that are often the case.

To finish, we have displayed an explicit transition of a system from the chaotic regime to the integrable one by means of the protocol we previously introduced, and conclude that it does indeed afford excellent results.

ACKNOWLEDGMENTS

This work has been supported by the Spanish Grants Nos. FIS2015-63770-P (MINECO/ FEDER) and PGC2018-094180-B-I00 (MCIU/AEI/FEDER, EU). The authors are grateful to L. Muñoz for enlightening discus-

sions.

-
- [1] H.J. Stöckmann, *Quantum Chaos* (Cambridge University Press, Cambridge, 1999).
- [2] M.V. Berry and M. Tabor, *Level clustering in the regular spectrum*, Proc. R. Soc. London A **356**, 375 (1977).
- [3] M. L. Mehta, *Random Matrices* (Academic Press, New York, 1991).
- [4] O. Bohigas, M.J. Giannoni, and C. Schmit, *Characterization of chaotic quantum spectra and universality of level fluctuation laws*, Phys. Rev. Lett. **52**, 1 (1984).
- [5] Y. Y. Atas, E. Bogomolny, O. Giraud, and G. Roux, *Distribution of the ratio of consecutive level spacings in random matrix ensembles*, Phys. Rev. Lett. **110**, 084101 (2013).
- [6] A. Relaño, J.M.G. Gómez, R.A. Molina, J. Retamosa, and E. Faleiro, *Quantum chaos and $1/f$ noise*, Phys. Rev. Lett. **89**, 244102 (2002).
- [7] E. Faleiro, U. Kuhl, R.A. Molina, L. Muñoz, A. Relaño, and J. Retamosa, *Power spectrum analysis of experimental sinai quantum billiards*, Phys. Lett. A **358**, 251 (2006).
- [8] M. Białous, V. Yunko, S. Bauch, M. Lawniczak, B. Dietz, and L. Sirko, *Power spectrum analysis and missing level statistics of microwave graphs with violated time reversal invariance*, Phys. Rev. Lett. **117**, 144101 (2016).
- [9] J.M.G. Gómez, A. Relaño, J. Retamosa, E. Faleiro, L. Salasnich, M. Vranicar, and M. Robnik, *$1/f^\alpha$ noise in spectral fluctuations of quantum systems*, Phys. Rev. Lett. **94**, 084101 (2005); A. Relaño, *Chaos-assisted tunneling and $1/f^\alpha$ spectral fluctuations in the order-chaos transition*, Phys. Rev. Lett. **100**, 224101 (2008).
- [10] E. Faleiro, J.M.G. Gómez, R.A. Molina, L. Muñoz, A. Relaño and J. Retamosa, *Theoretical derivation of $1/f$ noise in quantum chaos*, Phys. Rev. Lett. **93**, 244101 (2004).
- [11] J. M. G. Gómez, K. Kar, V. K. B. Kota, R. A. Molina, A. Relaño, and J. Retamosa, *Many-body quantum chaos: Recent developments and applications to nuclei*, Phys. Rep. **499**, 103 (2011).
- [12] R. Riser, V. A. Osipov, and E. Kanzieper, *Power spectrum of long eigenlevel sequences in quantum chaotic systems*, Phys. Rev. Lett. **118**, 204101 (2017).
- [13] J.M.G. Gómez, R.A. Molina, A. Relaño, and J. Retamosa, *Misleading signatures of quantum chaos*, Phys. Rev. E **66**, 036209 (2002).
- [14] L.F. Santos, *Integrability of a disordered Heisenberg spin-1/2 chain*, J. Phys. A: Math. Gen. **37** (2004) 4723-4729.
- [15] N.D. Chavda, H.N. Deota, and V.K.B. Kota, *Poisson to GOE transition in the distribution of the ratio of consecutive level spacings*, Physics Letters A **378** (2014) 3012-3017.
-

Appendix: Calculation of the theoretical power spectrum for the integrable case

In this section we give details on the calculations performed in Section III, for both the unfolded and the reunfolded cases.

1. Derivation for the unfolded spacings

In evaluating Eq. (6) the first step is to find the value of $\langle \delta_\ell \delta_m \rangle$. One expands this term to obtain

$$\langle \delta_\ell \delta_m \rangle = \sum_{i=1}^{\ell} \sum_{j=1}^m \langle (s_i - 1)(s_j - 1) \rangle = \sum_{i=1}^{\ell} \sum_{j=1}^m (\langle s_i s_j \rangle - \langle s_i \rangle - \langle s_j \rangle + 1). \quad (\text{A.1})$$

Concentrating on each of the terms separately yields

$$\sum_{i=1}^{\ell} \sum_{j=1}^m \langle s_i s_j \rangle = \sum_{i=1}^{\ell} \sum_{j=1}^m (\delta_{ij} + 1) = \min\{\ell, m\} + \ell m \quad (\text{A.2})$$

as well as

$$\sum_{i=1}^{\ell} \sum_{j=1}^m \langle s_i \rangle = \sum_{i=1}^{\ell} \sum_{j=1}^m 1 = \ell m = \sum_{i=1}^{\ell} \sum_{j=1}^m \langle s_j \rangle. \quad (\text{A.3})$$

Plugging Eqs. (A.2) and (A.3) into Eq. (A.1) one immediately obtains for the power spectrum the expression in Eq. (8). Summing over ℓ and m leads to

$$\langle P_k^\delta \rangle = \frac{1}{\sin^2(\omega_k/2)} \frac{1 + 2N - \cos(\omega_k N) + \frac{\sin(\omega_k N)}{\tan(\omega_k/2)}}{4N}, \quad (\text{A.4})$$

which is then rearranged to finally yield the result in Eq. (9). One must take the time to observe that such a leading order expression is indeed *inexact* when one considers an arbitrary value of N .

2. Derivation for the reunfolded spacings

We now consider Eq. (19). The calculation that follows is analogous to the previous one, but caution must be exercised since it becomes more cumbersome. First one considers as starting point the equation

$$\langle \tilde{\delta}_\ell \tilde{\delta}_m \rangle = \sum_{i=1}^{\ell} \sum_{j=1}^m \langle (\tilde{s}_i - 1)(\tilde{s}_j - 1) \rangle = \sum_{i=1}^{\ell} \sum_{j=1}^m (\langle \tilde{s}_i \tilde{s}_j \rangle - \langle \tilde{s}_i \rangle - \langle \tilde{s}_j \rangle + 1). \quad (\text{A.5})$$

We now take the easiest non-trivial element, i.e.,

$$\langle \tilde{s}_i \rangle = N \left\langle \frac{s_i}{\sum_{j=1}^N s_j} \right\rangle. \quad (\text{A.6})$$

To proceed, we make use of the fact that the nearest neighbor spacings are uncorrelated in an integrable system. Suppose each random variable \tilde{s}_i is distributed as $\tilde{s}_i \sim \text{Exp}(1)$, that is, \tilde{s}_i is a Poisson random variable with probability density f_i . One then has the N -dimensional integral for the mean i -th nearest neighbor reunfolded spacing given by

$$\begin{aligned} \langle \tilde{s}_i \rangle &= N \int_{\mathbb{R}^N} ds_1 \cdots ds_i \cdots ds_N \frac{s_i}{s_1 + \cdots + s_i + \cdots + s_N} f_i(s_1, \dots, s_i, \dots, s_N) \\ &= N \int_0^\infty ds_1 \cdots ds_i \cdots ds_N \frac{s_i}{s_1 + \cdots + s_i + \cdots + s_N} e^{-(s_1 + \cdots + s_i + \cdots + s_N)}. \end{aligned} \quad (\text{A.7})$$

This integral can be evaluated by changing to hyperspherical coordinates. Performing the above integral produces

$$\langle \tilde{s}_i \rangle = 1. \quad (\text{A.8})$$

We observe that $\langle \tilde{s}_i \rangle = \langle s_i \rangle$, $\forall i \in \{1, \dots, N\}$. This proves the re-unfolding process preserves the mean value of the nearest neighbor spacings. Clearly, $\langle s_j \rangle$ is calculated in the exact same manner and yields the same result.

Next we consider the re-unfolded nearest neighbor spacing correlation given by

$$\langle \tilde{s}_i \tilde{s}_j \rangle = N^2 \left\langle \frac{s_i s_j}{\sum_{k=1}^N \sum_{\ell=1}^N s_j s_\ell} \right\rangle. \quad (\text{A.9})$$

Eq. (A.9) requires considering two different cases: (a) $i = j$ and (b) $i \neq j$. For (a) one has

$$\langle \tilde{s}_i^2 \rangle = N^2 \left\langle \frac{s_i^2}{\sum_{k=1}^N \sum_{\ell=1}^N s_j s_\ell} \right\rangle = N^2 \int_0^\infty ds_1 \cdots ds_N \frac{s_i^2}{(s_1 + \cdots + s_N)^2} e^{-(s_1 + \cdots + s_N)} = \frac{2N}{N+1}, \quad (\text{A.10})$$

while for (b) this becomes

$$\langle \tilde{s}_i \tilde{s}_j \rangle = N^2 \left\langle \frac{s_i s_j}{\sum_{k=1}^N \sum_{\ell=1}^N s_j s_\ell} \right\rangle = N^2 \int_0^\infty ds_1 \cdots ds_N \frac{s_i s_j}{(s_1 + \cdots + s_N)^2} e^{-(s_1 + \cdots + s_N)} = \frac{N}{N+1}. \quad (\text{A.11})$$

Both cases (a) and (b) can be expressed compactly by setting

$$\langle \tilde{s}_i \tilde{s}_j \rangle = \frac{N(\delta_{ij} + 1)}{N+1}. \quad (\text{A.12})$$

Note that Eq. (A.12) is identical to Eq. (5b) in the limit $N \rightarrow \infty$. It is surprising that *this difference is responsible for the 2 factor that comes up in the power spectrum*. We shall now prove this.

Plugging Eqs. (A.6) and (A.12) into Eq. (A.5), we obtain Eq. (21):

$$\begin{aligned} \langle \tilde{\delta}_\ell \tilde{\delta}_m \rangle &= \sum_{i=1}^{\ell} \sum_{j=1}^m \left[\frac{N(1 + \delta_{ij})}{1 + N} - 1 \right] = \frac{N}{N+1} (\min\{\ell, m\} + \ell m) - \ell m \\ &= \frac{1}{N+1} (N \min\{\ell, m\} - \ell m). \end{aligned} \quad (\text{A.13})$$

The power spectrum Eq. (20) is therefore obtained straightforwardly inserting Eq. (A.13) in Eq. (19). To proceed, one must perform the two double sums that appear in it. The first one has already been calculated and yields the result Eq. (9) with the substitution $N \rightarrow N + 1$. The second sum is calculated to obtain

$$\begin{aligned} \frac{1}{N(N+1)} \sum_{\ell=1}^N \sum_{m=1}^N \ell m e^{i\omega_k(\ell-m)} &= \frac{e^{-i(N-1)\omega_k}}{N(N+1)(e^{i\omega_k} - 1)^4} \left[N + e^{2i(N+1)\omega_k} - (N+1)e^{i\omega_k} - (N+1)e^{i(1+2N)\omega_k} \right. \\ &\quad \left. - N(N+1)e^{i\omega_k} - N(N+1)e^{i(N+2)\omega_k} + 2(N^2 + N + 1)e^{i(N+1)\omega_k} \right]. \end{aligned} \quad (\text{A.14})$$

On using the corresponding value for each sum, Eq. (22) is eventually reached, after tedious but trivial algebra, as

$$\begin{aligned} \langle \tilde{P}_k^\delta \rangle &= \frac{N}{4(N+1)\sin^2(\omega_k/2)} + \mathcal{O}\left(\frac{1}{N}\right) = \frac{1}{4\sin^2(\omega_k/2)} - \frac{1}{4(N+1)\sin^2(\omega_k/2)} + \mathcal{O}\left(\frac{1}{N}\right) \\ &= \frac{1}{4\sin^2(\omega_k/2)} + \mathcal{O}\left(\frac{1}{N}\right). \end{aligned} \quad (\text{A.15})$$

It is worth noting that *all* the calculations in this appendix are *exact*. We conclude that the expressions usually used for the theoretical power spectrum in the integrable case are the leading order of the results here derived, and the expressions become exact as well when $N \rightarrow \infty$.
